Chinese Chemical Letters 32 (2021) 914–917

Contents lists available at ScienceDirect

Chinese Chemical Letters

journal homepage: www.elsevier.com/locate/cclet

Communication

Nitrogen-doped holey graphene nanoscrolls for high-energy and high-power supercapacitors

Feng Su[a,b], Shuanghao Zheng[a], Fangyan Liu[a], Xiong Zhang[c,e], Fangyuan Su[d,e], Zhong-Shuai Wu[a,*]

[a] Dalian National Laboratory for Clean Energy, Dalian Institute of Chemical Physics, Chinese Academy of Sciences, Dalian 116023, China
[b] University of Chinese Academy of Sciences, Beijing 100049, China
[c] Institute of Electrical Engineering, Chinese Academy of Sciences, Beijing 100190, China
[d] CAS Key Laboratory of Carbon Materials, Institute of Coal Chemistry, Chinese Academy of Sciences, Taiyuan 030001, China
[e] Dalian National Laboratory for Clean Energy, Chinese Academy of Sciences, Dalian 116023, China

ARTICLE INFO

Article history:
Received 3 June 2020
Received in revised form 8 July 2020
Accepted 9 July 2020
Available online 15 July 2020

Keywords:
Graphene nanoscrolls
Nitrogen doping
Holey grapheme
Supercapacitors
Ionic liquid

ABSTRACT

Porous structure and heteroatom doping are two key parameters for significantly boosting the capacitive performance of graphene-based materials. Herein, we report a facile approach to prepare one-dimensional (1D) nitrogen-doped holey graphene nanoscrolls (NHGNSs) through cold quenching treatment of two-dimensional graphene oxide sheets, followed by thermal annealing in the successive atmosphere of NH_3 and air. Benefiting from the synergy of the unique 1D tubular morphology, abundant nanoholes and nitrogen doping, the NHGNSs exhibit a high specific capacitance of 126 F/g at 1 A/g in ionic liquid electrolyte and excellent rate capability with 81% of the capacitance retained at 20 A/g. Furthermore, the fabricated symmetric supercapacitors based on NHGNSs achieve both high energy density of 53.5 Wh/kg at 875 W/kg and high power density of 17.5 kW/kg at 43.4 Wh/kg. The simple synthetic process and superior electrochemical performance suggest the great potential of NHGNSs for supercapacitor application.

Supercapacitors with the intriguing merits of fast charge delivery/storage, long lifespan, and excellent reliability have been demonstrated as a promising candidate for sustainable electrochemical energy storage, but the low energy density imposes substantial restrictions on their widespread application [1,2]. Therefore, increasing energy density without sacrificing power density has become one of the main challenges at present. In principle, the enhancement of energy density for electric double layer capacitors (EDLCs) can be realized through developing high-capacitance electrode materials working in electrolytes with wide stable potential window [3]. Owing to the unique combination of large specific surface area, high electrical conductivity, excellent mechanical properties and chemical stability, graphene has attracted extensive attention for electrochemical energy storage [4], and various graphene-based derivatives and composites have shown promise for high-performance supercapacitors [5–7].

Graphene nanoscrolls (GNSs) can be regarded as a new class of one-dimensional (1D) tubular graphene derivative obtained by continuous rolling of two-dimensional graphene sheets. In addition to inheriting the excellent properties of graphene, the unique 1D tubular structure of GNSs can avoid the restacking and agglomeration of graphene sheets during the fabrication process, and the relatively open structure also allows external molecules to enter the interlayer space [8]. So far, the reported preparation approaches of GNSs using graphene or graphene oxide (GO) as precursors mainly include ultrasonication-induced self-assembly [9], interface forces-driven formation [10], templated assembly [11] and cold quenching method [8,12].

The morphological advantages and open structure of GNSs make them potential host materials for charge storage in supercapacitors and batteries [13,14]. As a typical example, Gao and co-workers tested the specific capacitance of pure GNSs prepared by cold quenching [14], which display a high capacitance retention of ~80% from 1 A/g (~90 F/g) to 50 A/g in sulfuric acid electrolyte. Although the GNSs afford an outstanding rate capability, the specific capacitance still needs to be improved. For boosting the electrochemical performance, heteroatom doping (*e.g.*, N, B, S, P, F) [15–17] and holey structures with in-plane nanoholes [18,19] have been demonstrated as highly effective ways for graphene. The former can change the electronic structure and chemical

* Corresponding author.
E-mail address: wuzs@dicp.ac.cn (Z.-S. Wu).

https://doi.org/10.1016/j.cclet.2020.07.025
1001-8417/

properties of graphene [20], and the latter can enhance the ion diffusion kinetics [21]. Therefore, it is expected that these strategies would also contribute to the capacitive performance of GNSs.

Herein, we report the facile preparation of nitrogen-doped holey GNSs (NHGNSs) derived from GONSs synthesized by the cold quenching method for high-energy and high-power supercapacitors in ionic liquid electrolyte. The NHGNSs were obtained by thermal annealing of the GONSs in NH_3 atmosphere for nitrogen doping and subsequent controlled air etching process for in-plane mesopore creation. Benefiting from the synergy of nitrogen doping and holey structure, the NHGNSs exhibit significantly enhanced capacitance and rate capability compared with pure GNSs and nitrogen doped GNSs (NGNSs). More importantly, the fabricated NHGNSs-based symmetric supercapacitors provide high energy density of 53.5 Wh/kg and maintain 43.4 Wh/kg at high power density of 17.5 kW/kg.

A schematic illustration for the stepwise preparation of NHGNSs is presented in Fig. 1. First, the GONSs were synthesized by the cold quenching method in liquid nitrogen using hot aqueous dispersion of large-size GO sheets (Fig. S1a in Supporting information) as the precursor, followed by vacuum freeze-drying. Next, the GONSs were thermally annealed in NH_3 at 500 °C for simultaneous nitrogen doping and reduction to synthesize the NGNSs. Successively, the NGNSs were heated in air for a moderate carbon corrosion reaction. To determine the reaction condition, thermalgravimetric analysis (TGA, Fig. S2 in Supporting information) of the NGNSs was first conducted, which indicated that the calcination temperature should be lower than 390 °C to prevent excessive loss of carbon. Then, the reaction temperature was further optimized according to the weight retention after a heating duration of 5 h and controlled just below the threshold of dramatic weight loss to ensure efficient etching for in-plane hole formation. After the optimized air oxidation process at 360 °C, the NHGNSs were obtained with a yield of 83%–86% through the reaction between the defective sites of NGNSs and oxygen, in which the graphitic carbon was mostly maintained [19]. For comparison, the GONSs were also thermally annealed in N_2 at 800 °C to prepare the GNSs.

The morphology of the as-prepared samples was characterized by scanning electron microscopy (SEM) and transmission electron microscopy (TEM). As shown in Fig. 2 and Fig. S1 (Supporting information), the NHGNSs possess unique 1D tubular topology with diameters mainly ranging from 200 nm to 500 nm. It should be noted that a small amount of graphene sheets still exist in the final product. High-resolution TEM image (Fig. 2c) confirms the mesopore formation on the wall of NHGNSs. The topological open structure and the existence of in-plane holes can provide abundant pathways for ion migration and increase the accessible surface and edge for ion adsorption [21].

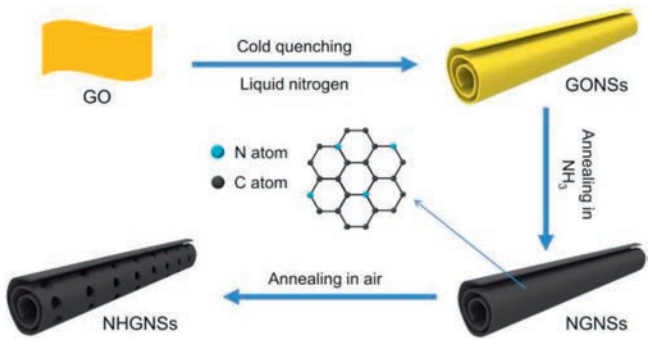

Fig. 1. Schematic illustration of the preparation of NHGNSs.

Fig. 3a shows the X-ray diffraction (XRD) patterns of the four samples. The diffraction peak of GONSs is located at 10.8°, corresponding to a d-spacing of 8.2 Å. After thermal treatment, the characteristic diffraction peaks (002) shift up to 26.5° for GNSs, 26.1° for NGNSs, and 26.2° for NHGNSs, indicative of the reduction of GONSs. The Raman spectra (Fig. 3b) show the typical broad D-band at around 1355 cm^{-1} and G-band at around 1600 cm^{-1} for all three samples. The intensity ratio of the D and G bands (I_D/I_G) is generally utilized as an index of the structural defects and the crystallinity of graphitic carbons. From Fig. 3b, the I_D/I_G ratios of GONSs, GNSs, NGNSs and NHGNSs are calculated to be 0.99, 1.00, 1.06 and 1.03, respectively. The slightly decreased I_D/I_G ratio of NHGNSs, in comparison with NGNSs, suggests the marginally improved graphitic crystallinity. This can be attributed to the further removal of defective carbon during the air etching process at moderate temperature [19].

X-ray photoelectron spectroscopy (XPS) was further performed to probe the chemical composition of GONSs and NHGNSs. Fig. 3c shows the full XPS spectra, in which characteristic peaks corresponding to C 1s and O 1s are observed for both samples. The C/O ratio of NHGNSs is about 7.1 (Table S1 in Supporting information), much higher than that of GONSs (~2.0) due to the reduction by NH_3 at high temperature. Moreover, an additional N 1s peak appears for NHGNSs, demonstrative of the successful incorporation of nitrogen atoms. Notably, the nitrogen content of NHGNSs is as high as 9.0 at% by XPS analysis. The high-resolution N 1s spectrum of NHGNSs (Fig. 3d) can be well fitted into three main peaks at 398.2, 399.7 and 401.2 eV, arising from pyridinic N, pyrrolic N and graphitic N, respectively. According to the fitting results, the percentages of pyridinic N, pyrrolic N and graphitic N in NHGNSs are calculated to be 23.6, 56.5, and 19.9 at%, respectively. The high doping level of nitrogen in graphene lattice may conduce to the enhancement of electrochemical performance.

To evaluate the capacitive performance of the above active materials, two-electrode symmetric cells were assembled using 1-ethyl-3-methylimidazolium tetrafluoroborate ($EMIMBF_4$) ionic liquid as electrolyte and measured within a high voltage of 3.5 V by cyclic voltammetry (CV), galvanostatic charge and discharge (GCD), and electrochemical impedance spectroscopy (EIS). The CV curves (Fig. 4a and Fig. S3 in Supporting information) display quasi-rectangular shape without distinct redox peaks, which show little distortion even at an ultrahigh scan rate of 1 V/s, indicative of excellent electrical double-layer charge storage. This typical capacitive behavior is also demonstrated by the triangle-shaped GCD profiles (Fig. 4b) measured at various current densities ranging from 1 A/g to 20 A/g (based on the mass of active material in a single electrode). According to the discharge segment of GCD curves, the NHGNSs deliver a high specific capacitance of 126 F/g at 1 A/g (Fig. 4c). Even at a high current density of 20 A/g, the NHGNSs can still provide 102 F/g with a remarkable retention rate of 81%, demonstrative of outstanding rate capability. In a sharp contrast, the GNSs measured under the same conditions (Fig. S4 in Supporting information) exhibit a low specific capacitance of 60 F/g at 1 A/g with only 51% of the capacitance retained at 20 A/g. Besides, the specific capacitance of the NGNSs (Fig. S5 in Supporting information) is 98 F/g at 1 A/g, and a capacitance retention of 65% is obtained at 20 A/g. The great improvement of both specific capacitance and rate capability of NHGNSs (Figs. 4c, d and Fig. S6 in Supporting information), in comparison with NGNs and GNSs, can be ascribed to the synergy of nitrogen doping and holey structure. The nitrogen doping is capable of modulating the surface chemistry and improving the electrode wettability [20]. Meanwhile, the holey structure can facilitate ion transport and increase accessible surface area [21]. The larger slope of NHGNSs-based supercapacitors in the low frequency region of EIS (Fig. S7 in Supporting information) further suggests the enhanced ion

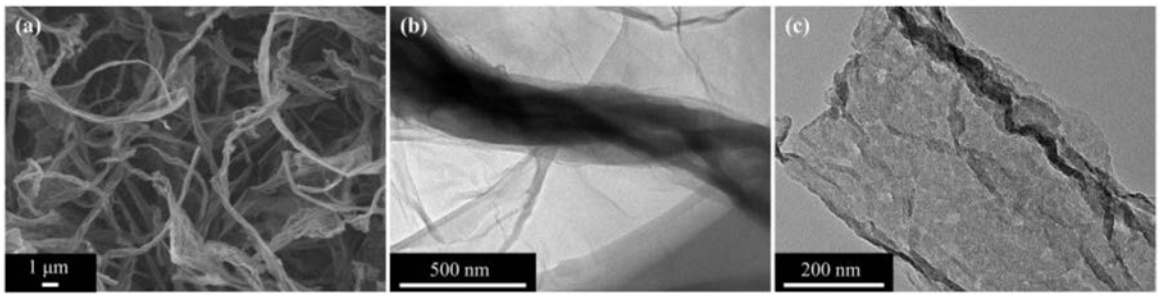

Fig. 2. (a) SEM and (b, c) TEM images of NHGNSs.

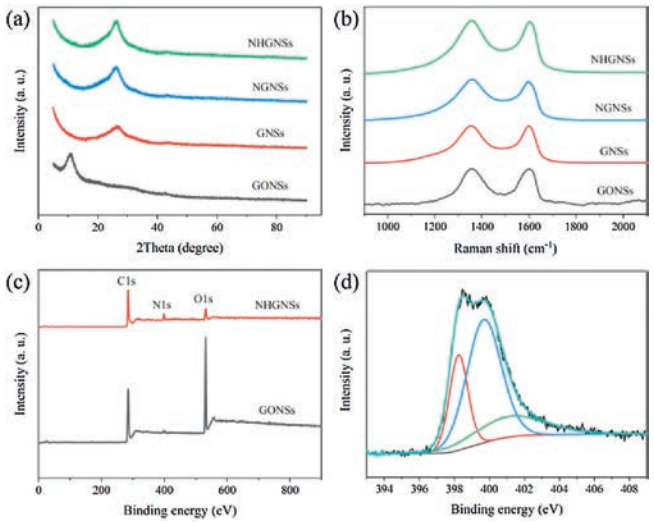

Fig. 3. (a) XRD patterns and (b) Raman spectra of NHGNSs, NGNSs, GNSs, and GONSs. (c) Overall XPS spectra of NHGNSs and GONSs. (d) N 1s XPS spectrum of NHGNSs.

diffusion kinetics. In addition, the slightly higher ohmic resistance of NHGNSs-based supercapacitors may originate from the little oxygen doping in the air oxidation process.

The energy densities and power densities of the symmetric supercapacitors based on NHGNSs, NGNSs and GNSs are calculated from the GCD profiles, and Ragone plot is presented in Fig. 4e. The NHGNSs-based supercapacitors achieve a high energy density of 53.5 Wh/kg at an average power density of 875 W/kg and still retain 43.4 Wh/kg at a high average power density of 17.5 kW/kg based on the mass of NHGNSs in the two electrodes, which is much better than the GNSs-based supercapacitors (25.5 Wh/kg at 875 W/kg and 12.9 Wh/kg at 17.5 kW/kg) and NGNSs-based supercapacitors (41.9 Wh/kg at 875 W/kg and 27.2 Wh/kg at 17.5 kW/kg) and also superior to many reported graphene- and carbon-based supercapacitors [22–27]. Furthermore, cycling stability was tested at a current density of 10 A/g, and the NHGNSs-based supercapacitors retain 91% of the initial capacitance with excellent coulombic efficiency of ~100% after 2000 cycles (Fig. 4f).

In summary, we have reported the facile production of NHGNSs through cold quenching of GO sheets and subsequent thermal annealing of GONSs in the successive atmosphere of NH_3 and air. When serving as electrode material for supercapacitors with ionic

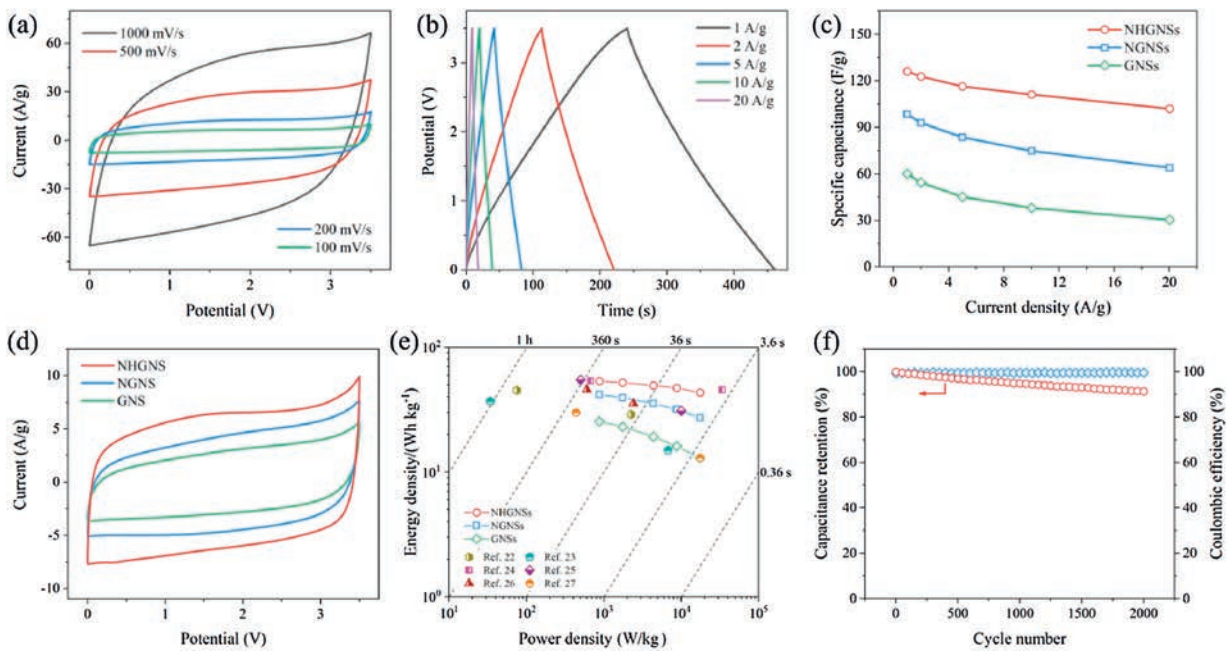

Fig. 4. Electrochemical performance of NHGNSs, NGNSs and GNSs for supercapacitors in $EMIMBF_4$ with a voltage of 3.5 V. (a) CV curves of NHGNSs obtained at various scan rates ranging from 100 mV/s to 1000 mV/s. (b) GCD profiles of NHGNSs measured at different current densities ranging from 0.5 A/g to 10 A/g. (c) Specific capacitances of

liquid electrolyte, the NHGNSs deliver a high specific capacitance of 126 F/g and excellent rate capability with 81% of the capacitance maintained from 1 A/g to 20 A/g. This electrochemical performance is superior to those of GNSs and NGNSs, demonstrative of the critical roles of nitrogen doping and holey structure for boosting the capacitive performance. More importantly, the assembled NHGNSs-based supercapacitors can offer a high energy density of 53.5 Wh/kg and retain 43.4 Wh/kg even at a high power density of 17.5 kW/kg, outperforming many reported graphene- and carbon-based supercapacitors. Therefore, it can be concluded that the unique structure enables NHGNSs a promising electrode material for supercapacitors and even other electrochemical energy storage devices.

Declaration of competing interest

The authors declare that they have no known competing financial interests or personal relationships that could have appeared to influence the work reported in this paper.

Acknowledgment

This work was financially supported by the National Natural Science Foundation of China (Nos. 51872283, 21805273), National Key R&D Program of China (Nos. 2016YBF0100100, 2016YFA0200200), Liaoning BaiQianWan Talents Program, LiaoNing Revitalization Talents Program (No. XLYC1807153), Natural Science Foundation of Liaoning Province, Joint Research Fund Liaoning-Shenyang National Laboratory for Materials Science (No. 20180510038), DICP (Nos. DICP ZZBS201708, DICP ZZBS201802), DICP&QIBEBT (No. DICP&QIBEBT UN201702), DNL Cooperation Fund, CAS (Nos. DNL180310, DNL180308, DNL201912, DNL201915).

Appendix A. Supplementary data

Supplementary material related to this article can be found, in the online version, at doi:https://doi.org/10.1016/j.cclet.2020.07.025.

References

[1] A. Noori, M.F. El-Kady, M.S. Rahmanifar, R.B. Kaner, M.F. Mousavi, Chem. Soc. Rev. 48 (2019) 1272–1341.
[2] J. Qin, Z.S. Wu, F. Zhou, et al., Chin. Chem. Lett. 29 (2018) 582–586.
[3] L.M. Da Silva, R. Cesar, C.M.R. Moreira, et al., Energy Storage Mater. 27 (2020) 555–590.
[4] H. Huang, H. Shi, P. Das, et al., Adv. Funct. Mater. 30 (2020) 1909035.
[5] X. Shi, S. Zheng, Z.S. Wu, X. Bao, J. Energy Chem. 27 (2018) 25–42.
[6] C. Peng, J. Yu, S. Chen, L. Wang, Chin. Chem. Lett. 30 (2019) 1137–1140.
[7] K. Zhang, X. Yang, D. Li, J. Energy Chem. 27 (2018) 1–5.
[8] Z. Xu, B. Zheng, J. Chen, C. Gao, Chem. Mater. 26 (2014) 6811–6818.
[9] C.A. Amadei, I.Y. Stein, G.J. Silverberg, B.L. Wardle, C.D. Vecitis, Nanoscale 8 (2016) 6783–6791.
[10] H. Li, J. Wu, X. Qi, et al., Small 9 (2013) 382–386.
[11] T. Sharifi, E. Gracia-Espino, H.R. Barzegar, et al., Nat. Commun. 4 (2013) 2319.
[12] J. Zhao, B. Yang, Z. Yang, et al., Carbon 79 (2014) 470–477.
[13] Z. Zhang, J. Zhao, J. Zhou, et al., Energy Storage Mater. 8 (2017) 35–41.
[14] B. Zheng, Z. Xu, C. Gao, Nanoscale 8 (2016) 1413–1420.
[15] F. Zhou, H. Huang, C. Xiao, et al., J. Am. Chem. Soc. 140 (2018) 8198–8205.
[16] Z.S. Wu, Y.Z. Tan, S. Zheng, et al., J. Am. Chem. Soc. 139 (2017) 4506–4512.
[17] X. Yu, C. Pei, L. Feng, Chin. Chem. Lett. 30 (2019) 1121–1125.
[18] H. Guo, L. Liu, Q. Dou, et al., Energy Storage Mater. 19 (2019) 338–345.
[19] Y. Lin, X. Han, C.J. Campbell, et al., Adv. Funct. Mater. 25 (2015) 2920–2927.
[20] H. Xu, L. Ma, Z. Jin, J. Energy Chem. 27 (2018) 146–160.
[21] Y. Zhang, Q. Wan, N. Yang, Small 15 (2019) 1903780.
[22] W. Qian, F. Sun, Y. Xu, et al., Energy Environ. Sci. 7 (2014) 379–386.
[23] X. Lin, H. Lou, W. Lu, et al., Chin. Chem. Lett. 29 (2018) 633–636.
[24] H.K. Kim, A.R. Kamali, K.C. Roh, K.B. Kim, D.J. Fray, Energy Environ. Sci. 9 (2016) 2249–2256.
[25] J. Tian, C. Cui, C. Zheng, W. Qian, Chin. Chem. Lett. 29 (2018) 599–602.
[26] A.G. Kannan, A. Samuthirapandian, D.W. Kim, J. Power Sources 337 (2017) 65–72.
[27] A. Xiang, S. Xie, F. Pan, et al., Chin. Chem. Lett. (2020), doi:http://dx.doi.org/10.1016/j.cclet.2020.04.058.